

Designing of cooling conditions for Si-Al microalloyed TRIP steel on the basis of DCCT diagrams

A. Grajcar ^{a,*}, W. Zalecki ^b, R. Kuziak ^b

^a Division of Constructional and Special Materials, Institute of Engineering Materials and Biomaterials, Silesian University of Technology, ul. Konarskiego 18a, 44-100 Gliwice, Poland

^b Institute for Ferrous Metallurgy, ul. K. Miarki 12, 44-100 Gliwice, Poland

* Corresponding author: E-mail address: adam.grajcar@polsl.pl

Received 12.02.2011; published in revised form 01.04.2011

Materials

ABSTRACT

Purpose: The aim of the research presented in the paper is to design the cooling routes after plastic deformation ensuring the multiphase structure with a high fraction of retained austenite on the basis of DCCT diagram for a new-developed Si-Al microalloyed TRIP steel.

Design/methodology/approach: The CCT and DCCT diagrams were developed. Eight variants of the thermo-mechanical processing were designed on the basis of the DCCT diagram. The thermomechanical processing consisted of a multi-stage compression and various cooling strategies in the $\gamma \rightarrow \alpha$ transformation range and isothermal holding temperature at a bainitic transformation region.

Findings: The usefulness of DCCT diagram for designing the thermomechanical processing conditions for TRIP steels was demonstrated. The fraction of ferrite and retained austenite are highly dependent on a cooling path applied in the $\gamma \rightarrow \alpha$ transformation region and a fraction of retained austenite especially on the isothermal holding temperature. The highest fraction of retained austenite as irregular grains located in a ferritic matrix and fine islands or interlath regions in bainitic regions were obtained at temperature of 400 and 450°C.

Research limitations/implications: To determine precisely a fraction of retained austenite, the X-ray investigations has to be applied additionally to the image analysis.

Practical implications: The designed cooling conditions are of great importance for the thermomechanical strategy for manufacturing the advanced high strength TRIP steels.

Originality/value: The thermomechanical processing was carried out for a new group of TRIP steels with Si partially replaced by Al and containing microadditions of Nb and Ti.

Keywords: Metallic alloys; TRIP steel; CCT diagram; DCCT diagram; Microalloying; Retained austenite; Multiphase structure; Thermo-mechanical processing

Reference to this paper should be given in the following way:

A. Grajcar, W. Zalecki R. Kuziak, Designing of cooling conditions for Si-Al microalloyed TRIP steel on the basis of DCCT diagrams, Journal of Achievements in Materials and Manufacturing Engineering 45/2 (2011) 115-124.

1. Introduction

Multiphase TRIP-aided steels belong to the most spectacular achievements of contemporary metallurgy in the field of advanced materials for automotive industry. They are C-Mn-Si, C-Mn-Si-Al and C-Mn-Al-type steels, composed of a soft ferritic matrix containing bainite and metastable retained austenite [1-9]. It has been shown that the strain-induced martensitic transformation of retained austenite (ca. 10-15%) gives rise to the excellent balance of strength and ductility. TRIP (Transformation Induced Plasticity) steels are produced by intercritical annealing of cold rolled sheets and isothermal holding in the range of bainitic transformation [4-10] or using the thermomechanical processing with controlled cooling path [11-21]. In recent years, there is a trend to reduce silicon content to avoid problems during industrial casting and galvanizing processes. New ideas of chemical composition design include alternative low-Si steels with increased Al content [7-10]. This approach enables to produce carbide-free bainite, similarly like in high-Si TRIP steels. However, loss in strength has to be compensated. Recently, the C-Mn-Al-(Mo)-(Nb)-(Ti) steels are one of the directions of further development of advanced high-strength steels (AHSS) [7-10,18].

Obtaining a desired fraction of retained austenite is achieved through the selection of adequate chemical composition and conditions of heat treatment or thermomechanical processing, where the temperature and time of isothermal bainitic transformation are the most important [12-20]. Detailed information on the chemical composition design, mechanical properties, technological cold forming and intercritical annealing of cold-rolled sheets can be found in literature [1-10]. Current state of the problem regarding thermo-mechanically processed sheets is much poorer and requires explanation of many phenomena that have a different character as distinct from sheets produced by cold rolling and intercritical annealing. A main problem in production of hot-rolled sheets is the multi-stage controlled cooling after finishing rolling [13-21].

Proper design of cooling after finishing rolling ensuring the desired fraction and morphology of individual constituents of multiphase structure requires adjusting the cooling conditions according to the CCT (Continuous Cooling Transformations) diagrams. Despite large number of investigated TRIP steels, very few CCT diagrams can be found in the literature [7-10,25,26]. The highest capability of multiphase microstructure formation is present in case of $\gamma \rightarrow \alpha$ and $\gamma \rightarrow$ bainite transformations shifted to short times, at simultaneous delay of pearlitic transformation start. It should be taken into account that shifting of $\gamma \rightarrow \alpha$ transformation to the left on CCT diagrams occurs together with increased content of Si, Al and P in steel, while C and Mn influence in the opposite direction (Fig. 1). Tsukatani et al. [26] noticed that increasing Mn content from 1.5 to 2wt. % results in a displacement of $\gamma \rightarrow \alpha$ transformation range to the right. Generally, it is unfavourable because obtaining the same fraction of ferrite requires the decrease of cooling rate after hot rolling. Finally, it can reduce a ferrite fraction and the C content in austenite, which is necessary for stabilization of γ phase to room temperature.

Silicon and aluminium increase A_{c3} temperature of steel (Fig. 1). In addition, Si shifts pearlitic transformation to the left, however C, Mn, Al, Mo, Cr, Ni, Nb and B influence in the opposite direction [10,25,26]. For example, the A_{c3} temperature of

low-carbon 0.15C-1.5Mn-1Si-1Al steel equals 1148°C [4,5] and for the medium-carbon 0.43C-1.5Mn-1Si-1Al-Nb-Ti steel its value is lowered to about 931°C [27]. It shows that - besides a beneficial effect for carbides hampering under isothermal bainitic transformation conditions - Si and Al make it possible to obtain a higher fraction of ferrite and to enrich austenite in carbon due to its diffusion into γ phase during $\gamma \rightarrow \alpha$ transformation.

The effect of Nb manifests by a slight increase of the $\gamma \rightarrow \alpha$ transformation temperature and advantageous shortening of time to initiate the transformation. For cold rolled TRIP steel sheets, at first some uncertainty concerned a hampering effect of niobium carbonitrides on the recrystallization progress under conditions of intercritical annealing.

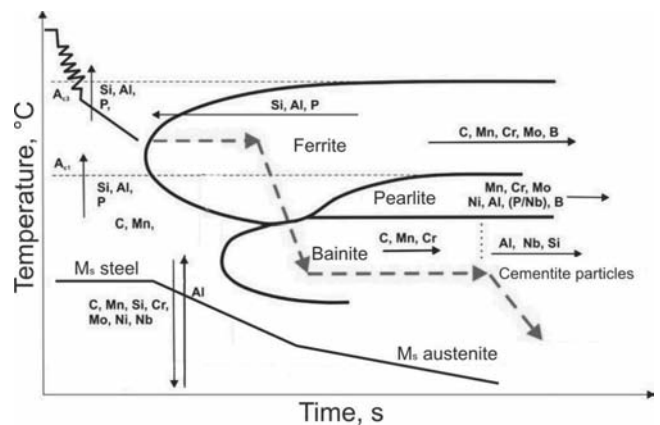


Fig. 1. Scheme of the influence of elements on the continuous cooling transformations diagram with a cooling path typical for TRIP-type sheets after hot rolling [10]

However, results obtained by DeArdo et al. [7] on C-Mn-Si-Al-Mo-Nb steels and by Fonstein et al. [9] on C-Mn-Al-Nb steels revealed that the presence of disperse particles of Nb(C,N) slightly affects the recrystallization kinetics.

The increase of martensite start temperature caused by Al has also to be taken into consideration. Its continuous decreasing during successive stages of heat treatment (Fig. 1) is necessary for stabilization of a required fraction of retained austenite below room temperature. Especially important for selection of proper conditions of multi-stage cooling for hot-rolled sheets are DCCT (Deformation Continuous Cooling Transformation) diagrams of supercooled plastically deformed austenite. Plastic deformation has a considerable influence on the shape of DCCT curves [21,27-29]. There is a lack of this type of diagrams for TRIP steels in literature yet.

2. Experimental procedure

The new-developed low-alloyed C-Mn-Si-Al-type steel with Nb and Ti microadditions was investigated. The steel contains: 0.24% C, 1.55% Mn, 0.87% Si, 0.4% Al, 0.034% Nb and 0.023% Ti. Chemical composition of elaborated steel was optimized with the aim of obtaining an optimal fraction of retained austenite under conditions of hot-working and controlled cooling.

In comparison to TRIP-type steels used most often, the developed steel is characterized by decreased to 0.87% concentration of silicon, which decrement was compensated by addition of Al. Moreover, the steel is characterized by high metallurgical purity connected to low concentration of phosphorus ($P=0.01\%$) and sulphur ($S=0.004\%$). The melt together with modification of non-metallic inclusions by rare-earth elements was done in the Balzers VSG-50 vacuum induction furnace at The Institute for Ferrous Metallurgy in Gliwice. Liquid metal was cast in the argon shield into ingot moulds with capacity of 25 kg. Successively, the ingots were hot forged into flat bars of 220 mm in width and 20 mm of thickness, from which the specimens for dilatometric tests and thermomechanical processing were machined.

Critical temperatures (A_{c3} and A_{c1}) of the investigated steel and diagrams of supercooled, non-deformed and plastically deformed austenite transformations were assigned using DIL805A/D dilatometer with the LVDT gauge head. Tubular samples, $\varnothing 4 \times 10$ mm, of 3 mm diameter hole were used for determination of CCT diagrams, while $\varnothing 4 \times 7$ mm cylindrical specimens for determination of DCCT diagrams after plastic deformation were applied. Thermal stabilization of the samples consisted in their heating at a rate of 10°C/s to the temperature of 650°C , at which they were held for 10 min and then cooled to ambient temperature at a rate of 0.5°C/s . After thermal stabilization, specimens were heated at a rate of 3°C/s to austenitizing temperature of 1100°C and held for 300 s. Subsequently, the samples were cooled at a rate of 5°C/s to the temperature of 900°C , being the start of controlled cooling or plastic deformation. Compression of cylindrical samples was conducted to the true strain of 0.69 and at the strain rate of 1 s^{-1} . Vickers hardness of samples cooled in a range from 600 to 1°C/s was measured with 100 N load. Microstructure observations of nital-etched specimens were carried out at magnification of 800x.

Developed CCT and DCCT diagrams were a basis to design the multi-stage cooling conditions for the specimens deformed in the thermomechanical simulator. The cuboidal specimens of $15 \times 20 \times 35$ mm were compressed under conditions of plane strain using DSI Gleeble 3800 simulator. After austenitizing at 1200°C for 30 s, the specimens were subjected to four-cycle compression. Ta foils were used to prevent sticking and graphite foils and Ni-based grease as lubricants. The hot-deformation conditions are given in Table 1. For a few variants, the deformation temperature of two final compression steps was decreased from 950 to 900°C and from 850 to 750°C . The results of the hot deformation behavior of the investigated steel are reported elsewhere [18, 30]. The present work is focused on designing the cooling conditions after hot deformation. The details of multi-stage cooling designed on the basis of DCCT diagram will be given in further chapters.

Table 1.

Parameters of the hot deformation conditions

	Deformation step			
	I	II	III	IV
Deformation	1150	1050	950 or 900	850 or 750
True strain	0.36	0.29	0.29	0.29
Strain rate, s^{-1}	7	8	9	10
Cooling rate	8	10	15	

After the thermo-mechanical treatment, samples for metallographic observations were machined. The specimens were prepared in the cross-section consistent with the direction of plastic flow. For the purpose of the best identification of retained austenite, etching in 10% water solution of sodium metabisulfite was applied. Two-stage etching (nital + sodium metabisulfite) was also used to reveal boundaries of ferrite grains. Metallographic observations were carried out using Leica MEF 4A optical microscope. The average fraction of ferrite and retained austenite (on a basis of 5 micrographs) was determined by the use of the Leica Qwin image analyzer.

3. Results and discussion

3.1. CCT and DCCT diagrams

The diagram of supercooled austenite transformations presented in Fig. 2a is necessary to design multi-stage cooling of steel from the temperature of deformation finish. The steel possesses the relatively high A_{c3} temperature, equal to 932°C . It is a result of high Al concentration in the steel and the influence of Nb and Ti microadditions. Martensite start temperature of the steel is equal to 360°C and it is relatively low despite increased concentration of Al in the steel. Cooling the steel at a rate of approximately 100°C/s results in obtaining the martensitic microstructure with hardness of around 490 HV. Bainitic region extended into a direction of short times guarantees obtaining bainitic-martensitic microstructures in a wide range of cooling rates, from about 100 to 20°C/s (Fig. 2a). As the example, the bainitic-martensitic microstructure of the steel cooled with a rate of 20°C/s is shown in Fig. 2b. Cooling at lower rates leads to the presence of ferrite in microstructure of the steel (Fig. 2c, d). Advantageous influence of Al and Si is stated by initiation of pearlitic transformation after approximately 70 s. For this reason, the time from the beginning of ferritic transformation to the beginning of pearlitic transformation is equal approximately 60 s. However, cooling of steel from the temperature of 900°C with a rate of 10°C/s causes obtaining nearly homogeneous microstructure of bainite. A decrease of cooling rate to 7°C/s does not also lead to achieving proper volume fraction of ferrite. Even cooling at the lowest rate not causing entering into a range of pearlitic transformation does not allow obtaining the desired fraction of ferrite (Fig. 2c). The small fraction of irregular ferrite is located only along primary austenite grains. This is caused by too short time for $\gamma \rightarrow \alpha$ transformation and, for instance, for cooling rate of 4°C/s , it is equal only 30 s. After cooling the steel at the rate of 2°C/s the microstructure contains bainite, a small fraction of ferrite and pearlite (Fig. 2d).

Plastic deformation essentially changes the shape of supercooled plastically deformed austenite transformations diagram (Fig. 3a). First of all, the overall refinement of the structure and the extension of the ferritic region can be observed. In particular, increase of the temperature of austenite into ferrite transformation occurs independent on a cooling rate of samples from the temperature of plastic deformation. Moreover, decrease of bainitic transformation start temperature and translation of ferritic bay to shorter time can be observed. Beginning of bainitic

transformation starts after 4 s. Displacement of pearlitic transformation in a direction of shorter time is also significant. Nevertheless, due to the acceleration of ferritic transformation, time for the end of $\gamma \rightarrow \alpha$ transformation is still equal 70 s. In practice, these factors create considerably higher chances of influencing the fraction and morphology of ferrite after hot rolling finish. A small fraction of acicular ferrite is present in the microstructure of steel deformed at 900°C already after cooling at the highest cooling rate applied equal 94°Cs⁻¹. Decrease of cooling rate to 20°Cs⁻¹ results in obtaining approximately 15% of fine-grained ferrite (Fig. 3b), while for non-deformed samples the same fraction of α phase was achieved after decreasing the cooling rate to 4°Cs⁻¹.

Increase of ferrite content to around 40% occurs together with a further decrease of cooling rate to 7°Cs⁻¹. Application of cooling rate being equal to 4°Cs⁻¹ leads to the initiation of pearlitic transformation (Fig. 3c). The fraction of pearlite rises along with a decrease of the cooling rate to 2°Cs⁻¹ (Fig. 3d). The increase of the ferrite fraction and significant refinement of the microstructure in a whole range of cooling rates were a result of considerable grow of the population of areas convenient for α phase nucleation, which are not only the boundaries of austenite grains but also deformation bands formed in plastically deformed austenite [11-17]. Optimum utilization of time for the $\gamma \rightarrow \alpha$ transformation requires the application of two-stage cooling regime after austenitizing.

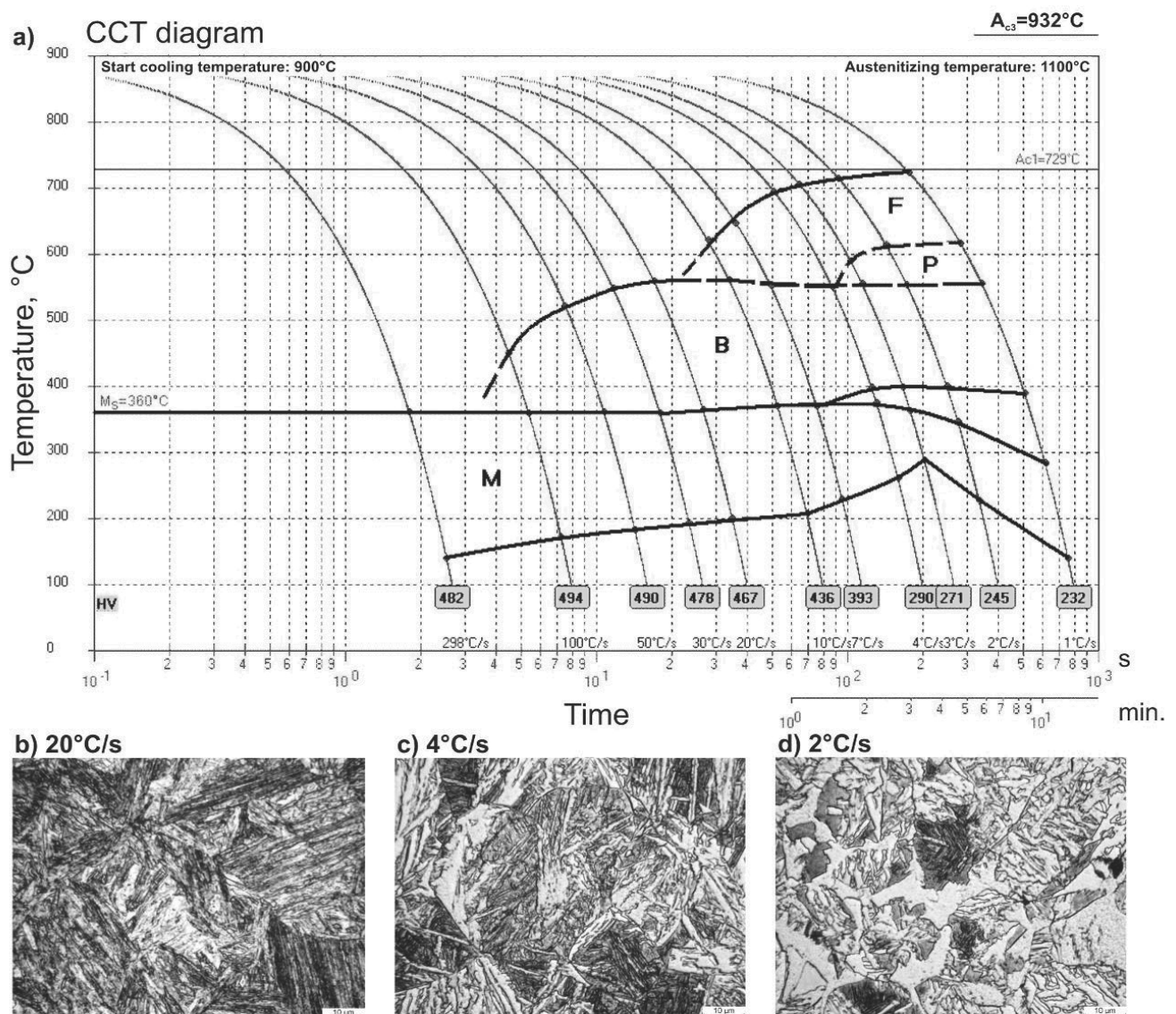


Fig. 2. The CCT diagram of the steel (a) and the structures obtained after cooling the specimens from the temperature of 900°C at a rate of: b) 20°C/s, c) 4°C/s and d) 2°C/s

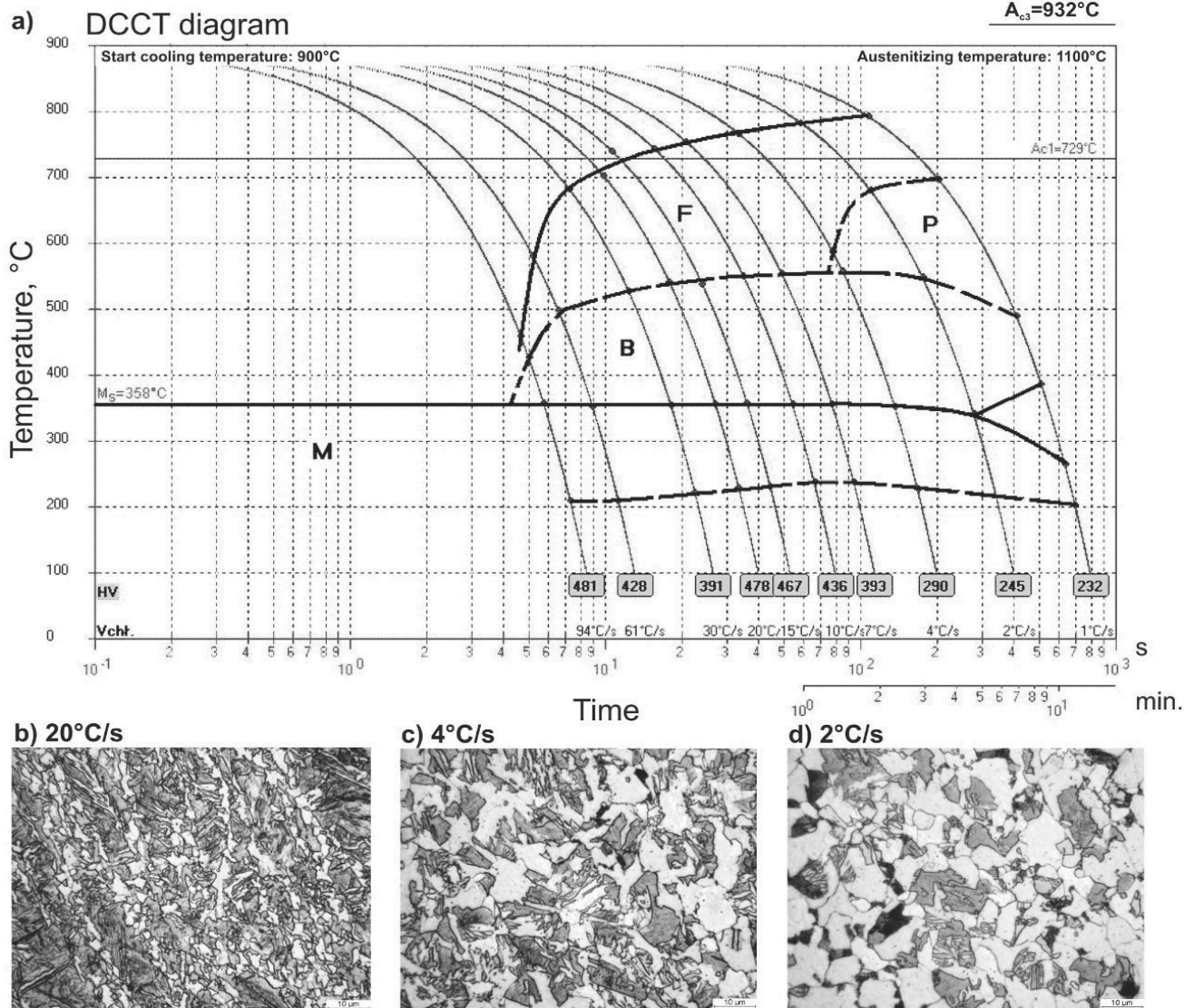


Fig. 3. The DCCT diagram of the steel (a) and the structures obtained after cooling the specimens from the deformation temperature of 900°C at a rate of: b) 20°C/s, c) 4°C/s and d) 2°C/s

3.2. Designing of cooling conditions on the basis of DCCT diagram

Obtaining multiphase structures containing a high fraction of retained austenite is highly dependent on a ferrite fraction and a morphology of bainite. These factors influence the redistribution of carbon during cooling and decide about austenite stability at room temperature. Eight variants of the cooling process were designed. The variants I-IV differ only in the temperature of isothermal holding of the steel in a bainitic range. The following were the goals of individual variants:

- Variants I-IV: cooling the specimen after plastic deformation at 850°C to temperature of 700°C with a rate of 15°C/s - corresponding to the cooling rate of the sheet with a thickness

of 2 mm in air - and subsequent slow cooling with a rate of 2°C/s in a range of the $\gamma \rightarrow \alpha$ transformation, guaranteeing optimal utilization of time for the diffusional transformation. To avoid pearlitic transformation, the next step consists of fast cooling at a rate of 40°C/s to the temperature of isothermal holding. The specimens were held for 600 s at 350, 400, 450 and 500°C and finally cooled at a rate of 0.5°C/s to room temperature.

- Variants V and VI: lowering the finishing deformation temperature to 750°C and omitting the initial air cooling. Taking into account an accelerating effect of temperature decreasing on the initiation of diffusive transformations - the cooling time in the $\gamma \rightarrow \alpha$ transformation range was shortened to 37 s (variant V) and 25 s (variant VI). The cooling rate was increased to 4°C/s. From the temperature of 600°C the cooling path was the same like in variants I-IV.

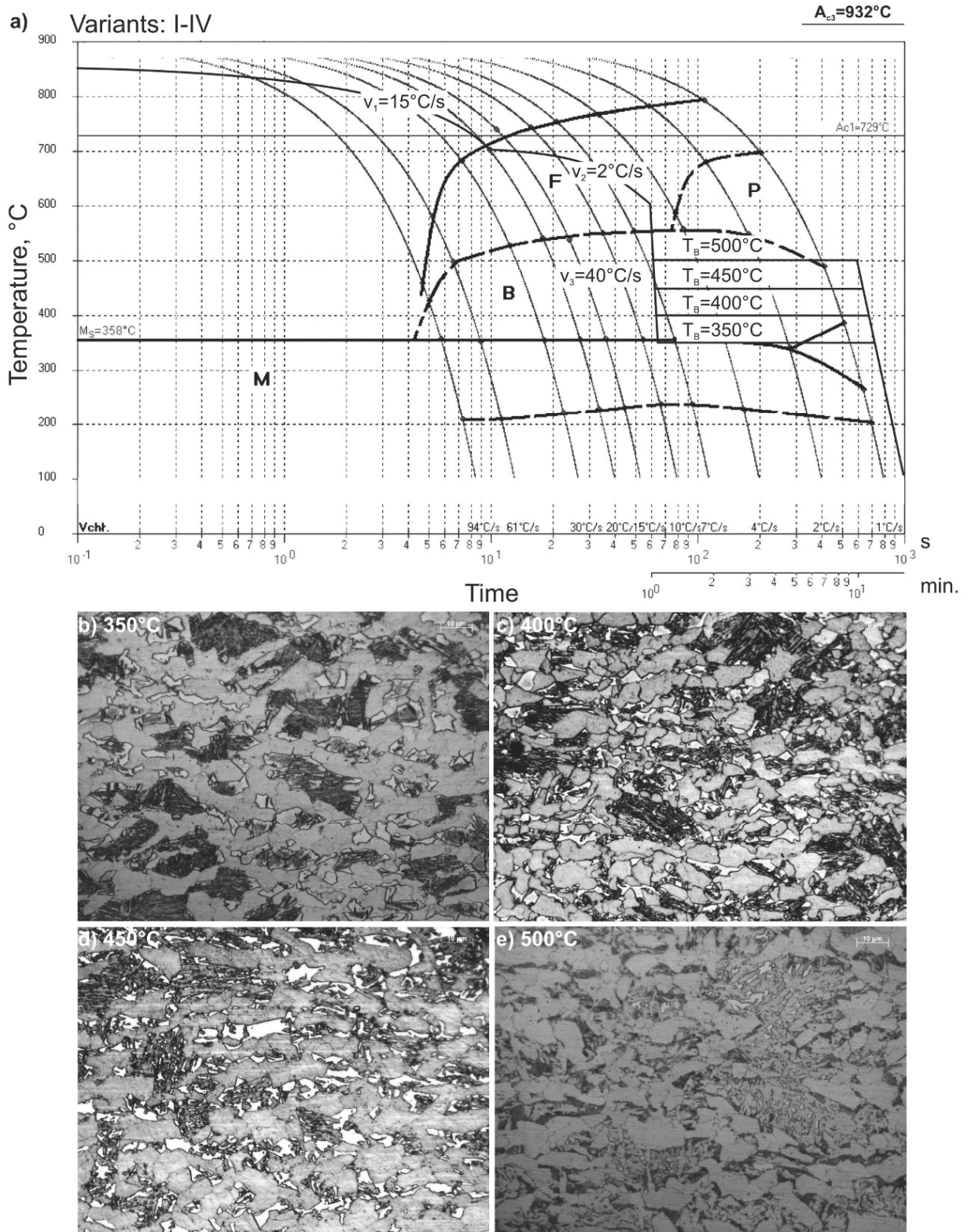


Fig. 4. Designed cooling conditions of variants I-IV plotted on the DCCT diagram of the steel (a) and the multiphase structures obtained after isothermal holding of specimens at temperature of 350°C (b), 400°C (c), 450°C (d) and 500°C (e)

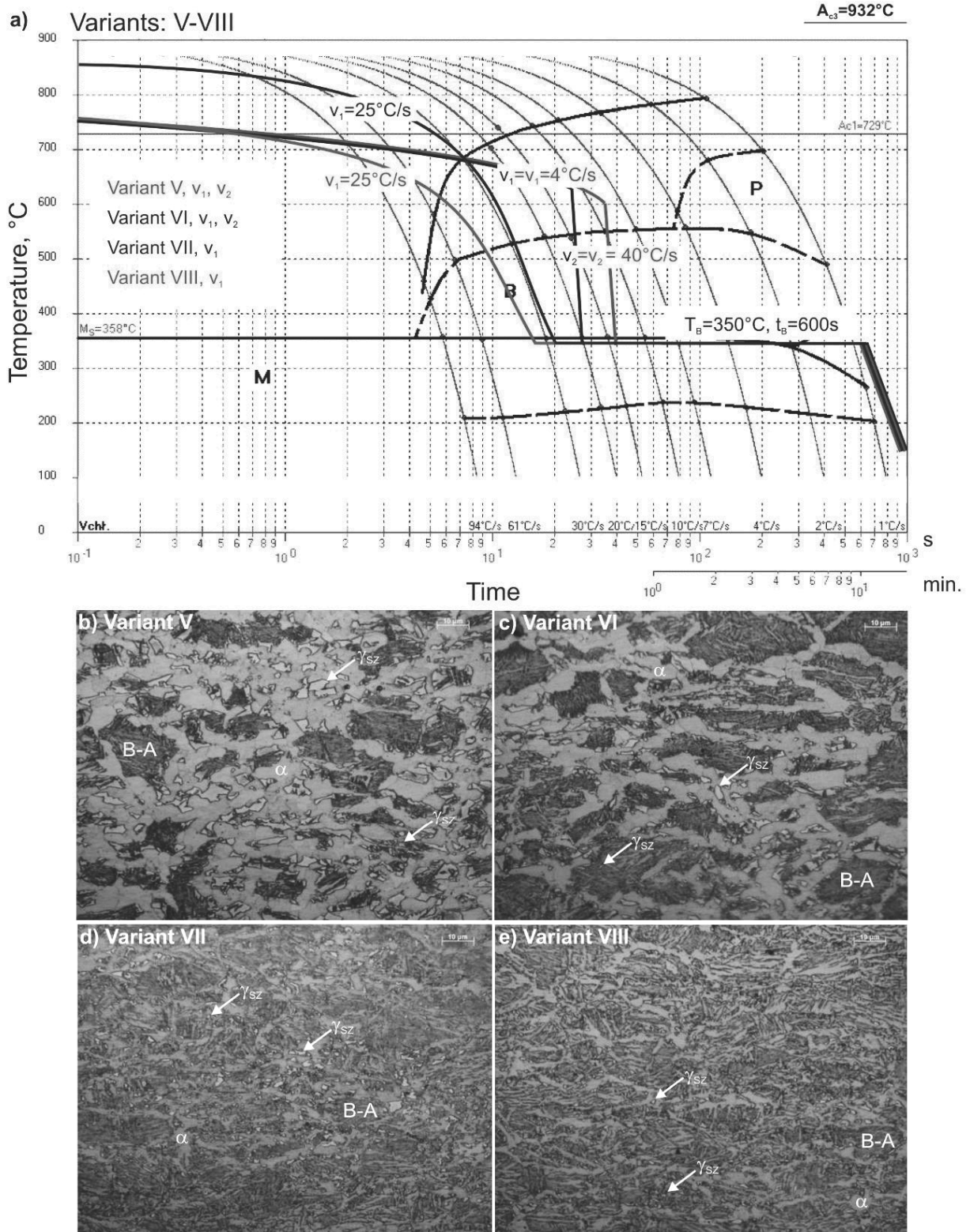


Fig. 5. Designed cooling conditions of variants V-VIII plotted on the DCCT diagram of the steel (a) and the multiphase structures obtained after various cooling of specimens in the $\gamma \rightarrow \alpha$ transformation range and isothermally held at temperature of 350°C (b-e)

- Variant VII: cooling the specimen from 850°C directly to the temperature of 350°C with a rate of 25°C/s without the necessity of slow cooling in the $\gamma \rightarrow \alpha$ transformation range.
- Variant VIII: lowering the finishing deformation temperature to 750°C and cooling the specimen directly to the temperature of 350°C with a rate of 25°C/s without the necessity of slow cooling in the $\gamma \rightarrow \alpha$ transformation range.

3.3. Multiphase structures obtained after the thermomechanical processing

Cooling curves described in the chapter 3.2 were superimposed on the DCCT diagram in Figs. 4 and 5. As a result of the conducted thermomechanical processing fine-grained ferritic-bainitic microstructures were obtained with a fraction of ferrite from 9 to 64% and the amount of retained austenite dependent on cooling route in the $\gamma \rightarrow \alpha$ transformation region and the temperature of isothermal holding in the bainitic range. Fig. 4 shows the microstructures obtained for the same cooling conditions in a ferritic range. For this reason, the ferrite fraction is nearly the same and equals about 63% (Table 2). It indicates that two-stage cooling is efficient to obtain much higher fraction of ferrite comparing to that obtained for a constant cooling rate at dilatometric experiments. According to the DCCT diagram (Fig. 4a), the cooling at a rate of 40°C/s precluded pearlite forming.

Table 2.
Fraction of retained austenite and ferrite for different variants of the thermomechanical processing

Variant	Designation	Austenite fraction, %		Ferrite fraction, %
		Image analysis	X-ray [19]	
I	850°C-15°C/s-700°C-50s-40°C/s-350°C	11.9±1.4	9.6	63.1±3.7
II	850°C-15°C/s-700°C-50s-40°C/s-400°C	14.1±0.6	16.0	62.3±4.0
III	850°C-15°C/s-700°C-50s-40°C/s-450°C	14.1±0.7	16.8	64.2±3.7
IV	850°C-15°C/s-700°C-50s-40°C/s-500°C	6.1±0.9	6.3	61.6±3.5
V	750°C-37s-40°C/s-350°C	13.8±0.8	14.3	43.2±2.9
VI	750°C-25s-40°C/s-350°C	10.8±1.2	12.5	34.5±4.1
VII	850°C-25°C/s-350°C	4.9±0.6	10.0	9.3±2.0
VIII	750°C-25°C/s-350°C	4.5±0.7	9.1	12.4±2.2

The difference in the retained austenite fraction for variants I-IV is only dependent on the temperature of isothermal holding in the bainitic transformation range. Uniformly distributed bainitic-austenitic islands with a diversified size are located in the ferritic matrix and in bainitic islands. A considerable part of austenite

grains located in ferrite and the part of bainitic regions are characterized with elongation in the direction of plastic flow, what indicates that they formed from the non-recrystallized austenite at temperature lower than recrystallization finish temperature of this phase (Figs. 4b-e). Isothermal holding of steel in the temperature of 350°C leads to achievement of retained austenite located mainly on grain boundaries of ferrite (Fig. 4b). Austenite in bainitic islands has undergone a total transformation and remains only in the boundary regions of the islands. The grains of γ phase have characteristic irregular shape and the equivalent diameter from 1 to 7 μm . Lamellar topography typical for martensite can be observed in some largest grains with a shape typical for austenite. The presence of martensite is a result of martensitic transformation occurring during the last cooling stage. The transformation indicates too low carbon enrichment of austenite due to relatively low isothermal holding temperature.

A considerable increase of isothermal holding temperature to 400°C results in increase of retained austenite fraction (Fig. 4c). There are no austenite grains transformed into martensite. It derives from decreasing M_s temperature of austenite below room temperature, what is reported in [19] on the basis of X-ray investigations. Apart from grains located in a ferritic matrix, the distinct increase of fine granules of retained austenite located in bainitic regions can be observed. A fraction of retained austenite in bainitic islands increases with a further rise of the isothermal holding temperature to 450°C (Fig. 4d). The total fraction of retained austenite estimated on a basis of image analysis is the highest and equals 14.1%, similarly to temperature of 400°C (Table 2).

A more detailed analysis of morphological features of retained austenite using SEM and EBSD technique carried out in [20] revealed that the γ phase in bainitic islands is present in a form of elongated thin layers or fine grains with sizes from 1 to 3 μm . It is visible that bainitic islands at temperature of 450°C are more fragmented (Fig. 4d) compared to that formed at lower temperatures (Figs. 4b,c). An increase of holding temperature to 500°C causes a considerable decrease of γ phase fraction to about 6% (Table 2) due to carbide precipitation. In such conditions, only fine grains of austenite located in bainitic islands are stable (Fig. 4e). They are probably characterized by higher concentration of carbon than the grains located on the boundaries of ferrite that have undergone a transformation into upper bainite or fine-lamellar pearlite.

The microstructures in Fig. 5 can be directly compared to the ones in Fig. 4b, because of the same isothermal holding temperature in a bainitic range. Lowering the finishing deformation temperature to 750°C leads to overall refinement of microstructure (Fig. 5b) compared to the specimens deformed at 850°C (Fig. 4b). The fraction of retained austenite increased to 13.8% (Table 2) as a result of its complex stabilization by grain size refinement, higher diffusion rate of carbon in highly deformed non-recrystallized austenite and increased dislocation density in retained austenite [11-17]. The γ phase grains occur mainly at grain boundaries of ferritic matrix. Shortening the time of slow cooling in the $\gamma \rightarrow \alpha$ transformation region to 37 s results in decreasing a ferrite fraction. It is visible more clearly with a further decrease of the time to 25 s, where the ferrite fraction decreases to about 35% (Table 2). A direct result of lower ferrite fraction is decreasing a fraction of retained austenite to 10.8% and

lower fragmentation of bainitic islands (Fig. 5c). Retained austenite grains and bainitic islands formed at 750°C are also more flattened comparing to these structural constituents formed at 850°C.

The lowest fraction of ferrite was obtained under conditions of continuous cooling of specimens with a rate of 25°C/s from a finishing deformation temperature of 850°C or 750°C (Table 2). It is connected to the application of fast cooling in the $\gamma \rightarrow \alpha$ region. As observed earlier, the lower ferrite fraction reflects in lower fraction of γ phase. However, it is not so obvious when considering the retained austenite determined in [19] by X-ray method (Table 2). The fraction of retained austenite determined in this way averages 10% and is just slightly lower compared to the variants V and VI, where two-stage cooling was applied. Twice larger austenite fraction for variants VII and VIII and lower differences for other variants of the thermomechanical processing determined by the X-ray method (Table 2) requires explanation.

For specimens cooled continuously from the finishing deformation temperature, retained austenite occurs as fine, uniformly distributed granules (Figs. 5d,e) located on ferrite-bainite boundaries and inside bainitic regions. As distinguished from other variants a large majority of retained austenite is a constituent of B-A islands. The understated fraction of γ phase for variants VII and VIII is a result of a lack of precise identification of finest granules and lamellar regions of retained austenite being a component of bainitic islands. This limitation is not valid for X-ray examination [19], which results should be acknowledged as the more representative than the image analysis.

A slightly lower fraction of retained austenite estimated by the image analysis compared to X-ray method for variants II-VI is because of the same reason (Table 2). In turn, the reason of a slightly overestimated fraction of γ phase for the variant I is treating as retained austenite of some fraction of martensite morphologically difficult to distinguish using only light microscopy. The etching quality of metallographic specimens strongly influences final results of distinguishing austenite and martensite. Analysing Fig. 5a it can be expected that the increase both in ferrite and retained austenite for the variants VII and VIII should occur with decreasing the cooling rate during the $\gamma \rightarrow \alpha$ transformation from 25 to about 7°C/s. However, taking into account the lower deformation temperature (850 or 750°C) compared to dilatometric tests (900°C) there is a risk to initiate pearlite transformation. The another way of increasing the austenite fraction - without changing amount of ferrite - is increasing the isothermal holding temperature to 400-450°C.

4. Conclusions

The investigated Si-Al microalloyed TRIP steel has a high potential to stabilize retained austenite, which is necessary to utilize TRIP effect during technological forming. CCT diagrams determined from the non-deformed austenite have a limited usefulness to design a cooling path after hot deformation guaranteeing a desired multiphase structure. Plastic deformation changes significantly a shape of austenite transformation diagrams and it is a main reason of the applying of DCCT diagrams. The possibility of forming the multiphase structure

after plastic deformation is high, especially due to the beneficial enlarging and shifting to short time of the $\gamma \rightarrow \alpha$ transformation region. A fraction of retained austenite is dependent on a fraction of ferrite but the more deciding condition is the isothermal holding temperature in a bainitic transformation range. The highest fraction of γ phase obtained when slow cooling in the $\gamma \rightarrow \alpha$ region was applied and the specimen was isothermally held at 400 or 450°C. At the temperature of 350°C retained austenite is present mainly in a form of irregular grains located on grain boundaries of ferrite and in the boundary regions of bainitic islands. After increasing the isothermal holding temperature to 400-450°C a large fraction of retained austenite occurs as fine granules or interlath regions in bainitic islands. These morphological forms of γ phase - difficult to unequivocal identification using light microscopy - occur also under conditions of continuous cooling from the finishing deformation temperature. At the temperature of 500°C the precipitation of carbides proceeds.

References

- [1] B.C. De Cooman, Structure-properties relationship in TRIP steels containing carbide-free bainite, *Current Opinion in Solid State and Materials Science* 8 (2004) 285-303.
- [2] R. Kuziak, R. Kawalla, S. Waengler, Advanced high strength steels for automotive industry, *Archives of Civil and Mechanical Engineering* 8/2 (2008) 103-117.
- [3] O. Muransky, P. Hornak, P. Lukas, J. Zrník, P. Sittner, Investigation of retained austenite stability in Mn-Si TRIP steel in tensile deformation condition, *Journal of Achievements in Materials and Manufacturing Engineering* 14 (2006) 26-30.
- [4] A.K. Lis, B. Gajda, Modelling of the DP and TRIP microstructure in the CMnAlSi automotive steel, *Journal of Achievements in Materials and Manufacturing Engineering* 15 (2006) 127-134.
- [5] B. Gajda, A.K. Lis, Intercritical annealing with isothermal holding of TRIP CMnAlSi steel, *Journal of Achievements in Materials and Manufacturing Engineering* 20 (2007) 439-442.
- [6] Z.C. Wang, S.J. Kim, C.G. Lee, T.H. Lee, Bake-hardening behaviour of cold-rolled CMnSi and CMnSiCu TRIP-aided steel sheets, *Journal of Materials Processing Technology* 151 (2004) 141-145.
- [7] A.J. DeArdo, J.E. Garcia, M. Hua, C.I. Garcia, A new frontier in microalloying: Advanced high strength coated sheet steels, *Materials Science Forum* 500-501 (2005) 27-38.
- [8] W. Bleck, K. Phiu-On, Microalloying of cold-formable multi phase steel grades, *Materials Science Forum* 500-501 (2005) 97-112.
- [9] N. Fonstein, O. Yakubovsky, D. Bhattacharya, F. Siciliano, Effect of niobium on the phase transformation behavior of aluminum containing steels for TRIP products, *Materials Science Forum* 500-501 (2005) 453-460.
- [10] B. Ehrhardt, T. Gerber, Property related design of advanced cold rolled steels with induced plasticity, *Steel Grips* 4 (2004) 247-255.

- [11] H.B. Ryu, J.G. Speer, J.P. Wise, Effect of thermomechanical processing on the retained austenite content in a Si-Mn Transformation-Induced-Plasticity steel, *Metallurgical and Materials Transactions A* 33A (2002) 2811-2816.
- [12] I.B. Timokhina, P.D. Hodgson, E.V. Pereloma, Effect of deformation schedule on the microstructure and mechanical properties of a thermomechanically processed C-Mn-Si transformation-induced-plasticity steel, *Metallurgical and Materials Transactions A* 34A (2003) 1599-1609.
- [13] A. Basuki, E. Aernoudt, Influence of rolling of TRIP steel in the intercritical region on the stability of retained austenite, *Journal of Materials Processing Technology* 89-90 (1999) 37-43.
- [14] I.B. Timokhina, P.D. Hodgson, E.V. Pereloma, Effect of microstructure on the stability of retained austenite in transformation-induced-plasticity steels, *Metallurgical and Materials Transactions* 35A (2004) 2331-2341.
- [15] L. Skalova, R. Divizova, D. Jandova, Thermo-mechanical processing of low-alloy TRIP-steel, *Journal of Materials Processing Technology* 175 (2006) 387-392.
- [16] Z. Li, D. Wu, Effects of hot deformation and subsequent austempering on the mechanical properties of Si-Mn TRIP steels, *ISIJ International* 46/1 (2006) 121-128.
- [17] H.J. Koh, S.K. Lee, S.H. Park, S.J. Choi, S.J. Kwon, N.J. Kim, Effect of hot rolling conditions on the microstructure and mechanical properties of Fe-C-Mn-Si multiphase steels, *Scripta Materialia* 38 (1998) 763-768.
- [18] A. Grajcar, Structural and mechanical behaviour of TRIP steel in hot-working conditions, *Journal of Achievements in Materials and Manufacturing Engineering* 30/1 (2008) 27-34.
- [19] A. Grajcar, H. Krztoń, Effect of isothermal bainitic transformation temperature on retained austenite fraction in C-Mn-Si-Al-Nb-Ti TRIP-type steel, *Journal of Achievements in Materials and Manufacturing Engineering* 35/2 (2009) 169-176.
- [20] A. Grajcar, Morphological features of retained austenite in thermo-mechanically processed C-Mn-Si-Al-Nb-Ti multiphase steel, *Journal of Achievements in Materials and Manufacturing Engineering* 39/1 (2010) 7-18.
- [21] J. Adamczyk, A. Grajcar, Structure and mechanical properties of DP-type and TRIP-type sheets obtained after the thermomechanical processing, *Journal of Materials Processing Technology* 162-163 (2005) 267-274.
- [22] W. Shi, L. Li, Ch. Yang, R.Y. Fu, L. Wang, P. Wollants, Strain-induced transformation of retained austenite in low-carbon low-silicon TRIP steel containing aluminum and vanadium, *Materials Science and Engineering A* 429 (2006) 247-251.
- [23] I.B. Timokhina, E.V. Pereloma, H. Beladi, P.D. Hodgson, A study of the strengthening mechanism in the thermo-mechanically processed TRIP/TWIP steel, *Proceedings of the 3rd International Conference on Thermomechanical Processing of Steels, Padua, 2008, 1-10.*
- [24] S. Hashimoto, S. Ikeda, K. Sugimoto, S. Miyake, Effects of Nb and Mo addition to 0.2%C-1.5%Si-1.5%Mn steel on mechanical properties of hot rolled TRIP-aided steel sheets, *ISIJ International* 44/9 (2004) 1590-1598.
- [25] M. Zhang, L. Li, R.Y. Fu, D. Krizan, B.C. De Cooman, Continuous cooling transformation diagrams and properties of micro-alloyed TRIP steels, *Materials Science and Engineering A* 438-440 (2006) 296-299.
- [26] I. Tsukatani, S. Hashimoto, T. Inoue, Effects of silicon and manganese addition on mechanical properties of high-strength hot-rolled sheet steel containing retained austenite, *ISIJ International* 31/9 (1991) 992-1000.
- [27] A. Grajcar, M. Opiela, Influence of plastic deformation on CCT-diagrams of low-carbon and medium-carbon TRIP steels, *Journal of Achievements in Materials and Manufacturing Engineering* 29/1 (2008) 71-78.
- [28] J. Adamczyk, M. Opiela, Influence of the thermo-mechanical treatment parameters on the inhomogeneity of the austenite structure and mechanical properties of the Cr-Mo steel with Nb, Ti and B microadditions, *Journal of Materials Processing Technology* 157-158 (2004) 456-461.
- [29] A.K. Panda, R.I. Ganguly, D.S. Sarma, R.Ch. Gupta, S. Misra, Effect of thermomechanical treatment on structure and mechanical properties of Mo-bearing dual phase steel, *Steel Research* 66 (1995) 309-317.
- [30] A. Grajcar, M. Opiela, Microstructure evolution in thermomechanically processed TRIP-type microalloyed steel, *Proceedings of the 3rd International Conference on Thermomechanical Processing of Steels, Padua, 2008, 1-11.*